arXiv:1207.4728v1 [astro-ph.HE] 19 Jul 2012

Analytic Solution for Self-regulated Collective Escape of Cosmic Rays from their Acceleration Sites

M.A. Malkov and P.H. Diamond[1]

CASS and Department of Physics, University of California, San Diego, La Jolla, CA 92093

mmalkov@ucsd.edu, pdiamond@ucsd.edu

R.Z. Sagdeev

University of Maryland, College Park, Maryland 20742-3280, USA

F.A. Aharonian

Dublin Institute for Advanced Studies, 31 Fitzwilliam Place, Dublin 2, Ireland

Max-Planck-Institut fï¿œr Kernphysik, PO Box 103980, 69029 Heidelberg, Germany

I.V. Moskalenko

Hansen Experimental Physics Laboratory, Stanford University, Stanford, CA 94305

Abstract

Supernova remnants (SNRs), as the major contributors to the galactic cosmic rays (CR), are believed to maintain an average CR spectrum by diffusive shock acceleration (DSA) regardless of the way they release CRs into the interstellar medium (ISM). However, the interaction of the CRs with *nearby* gas clouds crucially depends on the release mechanism. We call into question two aspects of a popular paradigm of the CR injection into the ISM, according to which they *passively* and *isotropically* diffuse in the prescribed magnetic fluctuations as test particles. First, we treat the escaping CR and the Alfvï¿œn waves excited by them on an equal footing. Second, we adopt field aligned CR escape outside the source, where the waves become weak. An exact analytic self-similar solution for a CR "cloud" released by a dimmed accelerator strongly deviates from the test-particle result. The normalized CR partial pressure may be approximated as $\mathscr{P}(p,z,t) = 2\left[|z|^{5/3} + z_{\rm dif}^{5/3}(p,t)\right]^{-3/5} \exp\left[-z^2/4D_{\rm ISM}(p)t\right]$, where p is the momentum of CR particle, and z is directed along the field. The core of the cloud expands as $z_{\rm dif} \propto \sqrt{D_{\rm NL}(p)t}$ and decays in time as $\mathscr{P} \propto 2z_{\rm dif}^{-1}(t)$. The diffusion coefficient $D_{\rm NL}$ is strongly suppressed compared to its background ISM value $D_{\rm ISM}$: $D_{\rm NL} \sim D_{\rm ISM}\exp(-\Pi) \ll D_{\rm ISM}$ for sufficiently high field-line-integrated CR partial pressure, Π. When $\Pi \gg 1$, the CRs drive Alfvï¿œn waves efficiently enough to build a *transport barrier* ($\mathscr{P} \approx 2/|z|$ -"pedestal") that strongly reduces the leakage. The solution has a spectral break at $p = p_{\rm br}$, where $p_{\rm br}$ satisfies the following equation $D_{\rm NL}(p_{\rm br}) \simeq z^2/t$.

[1]Also at WCI Center for Fusion Theory, NFRI, Korea

1. Introduction

The generation of cosmic rays (CR) in supernova remnant (SNR) shocks by the diffusive shock acceleration (DSA) mechanism (e.g., Drury *et al.* 2001) is understood reasonably well up to the point of their escape into SNR surroundings. But making this mechanism responsible for the most of galactic CRs requires understanding of all stages of the CR production including their escape from the accelerators. In fact, best markers for "CR-proton factories" are nearby molecular clouds (MC) illuminated by protons leaking from SNRs. CRs will be visible in gamma rays generated by collisions with protons in the cloud Aharonian *et al.* (1994); Aharonian and Atoyan (1996); Aharonian *et al.* (2008); Gabici *et al.* (2009); Tavani *et al.* (2010); Abdo *et al.* (2010b,a); Giuliani *et al.* (2011); Ellison and Bykov (2011); Torres *et al.* (2011). Whether this gamma radiation is detectable with the current instruments, depends on the CR leakage rate from the source. The recent surge in measurements of gamma-bright SNR suggests that the sensitivity threshold have already been crossed for at least several galactic SNRs and it is becoming increasingly timely to improve our understanding of the CR leakage from these objects.

Without such improvement, it is also difficult to resolve the ongoing debates about the primary origin of gamma-emission from some of the gamma-active remnants, e.g., RX J 1713 (e.g., Funk 2012; Inoue *et al.* 2012). In arguing for hadronic or leptonic origin, one needs to know exactly how far the CRs are spread from the source at a given time and with what spectrum. Indeed, strong self-confinement of accelerated CR may keep their flux through a remote MC below the instrument threshold, primarily (and counterintuitively) for powerful accelerators. Conversely, the self-confinement will enhance illumination of nearby MCs, thus enhancing the odds of detecting the hadronic contribution to the emission. Apart from the distance to the target MC, equally important is its magnetic connectivity with the CR source. Overall, the predictions for the emissivity of MCs near strong CR sources can differ from the test-particle results by an order of magnitude or more.

To better understand the physics of CR confinement to SNRs, in this paper we consider the CR escape separately from their acceleration which is assumed to have faded because of the SNR age. Specifically, we will formulate the problem as a diffusion of a CR cloud (CRC) released from an accelerator into the ISM and propagating through a 'gas' of self-excited Alfven waves. At the scales larger than the initial size of the cloud, the solution, after an adjustment to the local environments, will become self-similar to depend only on the background diffusivity $D_{\rm ISM}$ and the integrated CRC energy (cf. Sedov-Taylor solution for the point explosion).

The idea that the CRC confinement should be thought of as a *self-confinement* is not new (e.g., Wentzel 1974; Achterberg 1981). However, the analytic solution for CR propagation uniformly valid in both the nearby and far zones of the initial CRC seems to be unknown. This paper is aimed at presenting and analyzing such solution. With some reservations, it may also be applied to a late stage of CR acceleration in a SNR, when the particles become disconnected from the shock and diffuse outwards. Their pressure, however, should still be sufficient to drive strong Alfvén waves which limit their escape. We begin with a brief discussion of the problems with the current escape models, thus motivating the new one.

1.1. The need for a new CR escape model

Traditionally, the transport of CR is treated differently inside and outside a DSA accelerator. Outside, CR are thought to escape as *test particles* with a diffusion coefficient inferable from observations. This picture cannot be correct near the accelerator because the CR transport must be in a *self-confinement* regime, in which the CR streaming instability diminishes their diffusion coefficient by orders of magnitude. This CR anisotropy instability, and particularly its nonresonant extensions, macroscopically driven by the CR current and the CR pressure gradient, have a potential to generate magnetic field fluctuations well in excess of the ambient magnetic field, $\delta B \gtrsim B_0$ (e.g., Bell 2004; Drury and Falle 1986; Bykov *et al.* 2009; Malkov *et al.* 2010). At the very least, such strong fluctuations should justify the standard DSA assumption about the Bohm diffusion regime with the mean free path, (mfp) of the order of the particle gyroradius, r_g, achieved at $\delta B \sim B_0$. Naturally, the transport is isotropic in this regime. The ISM background turbulence, on the other hand, is much weaker $\delta B^2/B_0^2 \lesssim 10^{-5}$ at the CR relevant length scales, thus resulting in the CR mfp $\gtrsim 10^5 r_g$ (for GeV particles, or $r_g \gtrsim 10^{12}$cm). It is important to emphasize that under these circumstances the cross-field diffusion coefficient, $\kappa_\perp$ is suppressed by a large factor compared to the diffusion along the field line, $\kappa_\parallel$, i.e. $\kappa_\perp/\kappa_\parallel \sim (\delta B/B_0)^4$ (see, e.g., Drury 1983).

It follows then that there is a problem of describing particle transport between the self-confinement (accelerator vicinity) and the test-particle (far from accelerator) transport regimes. To circumvent this problem, the acceleration process has been treated separately from the particle escape using one of the two devices: the upper cut-off momentum and the free escape boundary (FEB) (see e.g., Reville *et al.* 2009; Drury 2011, for recent discussions). As the names suggest, accelerated particles escape instantly upon reaching a prescribed boundary either in momentum or in configuration space. Their escape is assumed to have no effect on the acceleration other than through the modification of the shock structure (e.g., Moskalenko *et al.* 2008). In a simplified visualization of the DSA as a 'box' process, for example (Drury *et al.* 1999), the upper cutoff and the FEB are two sides of the box in the particle phase space. There were efforts to include self-generated waves into the description of particle acceleration and escape from strongly modified CR shocks (Malkov *et al.* 2002; Malkov and Diamond 2006), or in numerical treatments (Galinsky and Shevchenko 2007, 2011; Fujita *et al.* 2011). In most approaches, however, a sudden jump in the CR diffusion coefficient in momentum space is introduced to set an upper cutoff, (e.g., Ptuskin and Zirakashvili 2005; Yan *et al.* 2012). Similar jump in coordinate space would result in a FEB.

As long as the CR transport outside the accelerator is treated in the test particle approximation, no smooth transition between the CR acceleration and their escape is provided, regardless of the scenario for the latter. But, the diffusion coefficient rises by roughly five orders of magnitude in a transition zone that should be correspondingly large, unlike an infinitely thin FEB. It is this zone where the CR escape flux and confinement time are set by self-generated waves, thus rendering the FEB a rather implausible concept. For many SNRs it is then not yet possible to conclude whether the gamma-emission is leptonic or hadronic, should such conclusion depend on the CR escape and on the subsequent illumination of adjacent clouds. In a broader sense, there is a missing link in galactic CR generation between the CR acceleration (under a very strong self-generated wave-particle scattering) and their subsequent propagation (in a very weak interstellar turbulence). The goal of this paper is to establish such link.

Our treatment below is applicable to the following two situations. In one situation, a shock accelerates particles continuously but some of them reach far enough or diffuse across the local field to become disconnected from the shock front and have thus chances to escape. While doing so, they drive their own waves at

a gyroradius scale, whose amplitudes gradually decrease outwards and so does the particle density. The second situation is a clear-cut case for this paper that deals with a CRC released into the ISM with no ongoing acceleration inside the CRC. Both situations correspond to a mesoscale transport regime that is intermediate between the Bohm diffusion inside the accelerator and a global, quasi-isotropic CR diffusion in the Galaxy, where a random large scale component of the galactic magnetic field at the scale of tens of parsecs should be distinguished from the regular, spiral arm aligned toroidal field Brunetti and Codino (2000); Strong *et al.* (2007); Blasi and Amato (2012). In the mesoscale transport regime, however, both components are considered as a large scale ambient field with a scale much larger than the CR gyroradius. Before we describe the next section the physical setting of the problem, it is worthwhile to emphasize some of the qualitative results. .

First of all, for sufficiently high initial CR pressure (higher than magnetic pressure) and low ambient turbulence level, $\delta B \ll B_0$, the spreading of the CRC strongly deviates from the usual test-particle solution. Instead of being controlled by only one (diffusive) scale $l_{\rm D} \sim \sqrt{D_{\rm ISM} t}$, the structure of the expanding CRC is more complicated. Namely, it comprises three zones, of which only the outermost has the above scaling but, significantly lower CR pressure. Conversely, the CR pressure in the innermost part remains strongly enhanced. The both zones are connected by a self-similar, $1/z$ CR pressure profile.

2. CR Escape Model

After the Sedov-Taylor (ST) expansion stage in which the shock radius increases as $R_{\rm s} \propto t^{2/5}$ and particularly in and after the so-called pressure driven snowplow stage with a slower expansion at or below $R_{\rm s} \propto t^{0.3}$ (e.g., Bisnovatyi-Kogan and Silich 1995; Truelove and McKee 1999), the diffusive propagation of CR away from the shock becomes more important than their bulk expansion driven by the overpressured SNR interior. Regardless of the escape mechanism, one of the most important parameters is the number of spatial dimensions involved (see, e.g., Drury 2011 for a recent discussion). Indeed, the 3D random walk is non-recurrent, so only the finite shock radius gives particle a chance to return to it. However, 2- and 1-D random walks are recurrent. Therefore, the first important assumption to make is, indeed, about the process dimensionality which immediately translates into the choice of magnetic field configuration. Note that since particles recede from the shock as $\bar{R} \propto t^{1/2}$, they escape already at the Sedov-Taylor stage.

Contrary to the recent analytic (Drury 2011; Ohira *et al.* 2011; Yan *et al.* 2012) and numerical (with self-driven Alfvén waves Fujita *et al.* 2011) treatments of the spherically symmetric particle escape, we consider an escape through the local flux tube. This choice is suitable for a SNR expansion in an ISM with a distinct large scale magnetic field direction that does not change very strongly on the SNR scale. As we stated in the Introduction, our goal is to fill the gap between the weak scattering propagation far away from the remnant and the Bohm diffusion regime near the shock, with $\kappa = \kappa_{\rm B}$. The perpendicular diffusion in the far zone is of the order of $\kappa_\perp \sim (\delta B/B_0)^4 \kappa_\parallel \ll \kappa_\parallel \ll \kappa_{\rm B}$, so that we may safely assume that in the unperturbed ISM the propagation is one-dimensional, along the field line.

Closer to and inside the accelerator (or rather in the region of its past activity), $\kappa_\perp \sim \kappa_\parallel \sim \kappa_{\rm B}$, which favors the isotropy assumption. However, we may integrate (average) the equations for the CR transport and wave generation across the magnetic field, assuming that there is no strong expansion of the CRC in this direction. The resulting problem reduces then to a largely one dimensional propagation along the field line (cf. e.g. Rosner and Bodo 1996; Ptuskin *et al.* 2008, where a field aligned propagation from CR sources has

also been adopted). A cartoon example of the basic configuration is shown in Fig.1.

The second important assumption to make is about the spatial arrangement of the initial CR population. As shown in Fig.1, we adhere to the idea that the acceleration is most efficient in the quasi-parallel shock geometry. It can be advocated on the theoretical grounds (Malkov and Völk 1995; Völk *et al.* 2003) and is also supported by PIC simulations (e.g., Gargaté and Spitkovsky 2012). Therefore, we may assume, for example, that two 'polar cusps' of accelerated particles are left behind after the acceleration has either faded out or entered its final stage when particles escape faster then they are replenished by the acceleration. It is tempting to consider the SN 1006 as a prototype of such geometry, but the similarity is physically not quite convincing, given the young age of the latter source. On the other hand, older remnants, such as W44, do show (Uchiyama *et al.* 2012) a bipolar CR escape that can also be attributed to the field aligned escape.

During earlier, more active stages of acceleration, CR presumably fill up both the downstream and upstream regions near the shock. Meanwhile, the contact discontinuity (CD) behind the cloud of accelerated CRs must have undergone the Rayleigh-Taylor instability with strong magnetic field enhancement (Gull 1973). The CD expansion at late evolution stages should thus act as a piston on the previously accelerated CRs. Note that the CR reflecting piston was already employed in numerical acceleration schemes, e.g., (Berezhko 1996), which might, however, somewhat overestimate the maximum CR energy (Kirk and Dendy 2001). In the post acceleration stage, and given the significant field amplification at the CD, it is reasonable to assume that CRs are partially coupled to the slowly expanding flow with the reflecting magnetic piston behind but while escaping upstream they couple to the ISM and diffuse away.

2.1. Basic equations, initial and boundary conditions

Perhaps the most systematic quasilinear derivation of equations for the coupled evolution of CR and Alfven waves is given by Skilling (1975). We use them in a simplified one-dimensional (along the ambient field, z-coordinate, Fig.1) form equivalent to that used by, e.g., Bell (1978) and, with an interesting "beyond quasilinear" interpretation, by Drury (1983)

$$\frac{d}{dt}P_{\rm CR}(p) = \frac{\partial}{\partial z}\frac{\kappa_{\rm B}}{I}\frac{\partial P_{\rm CR}}{\partial z} \tag{1}$$

$$\frac{d}{dt}I = -C_{\rm A}\frac{\partial P_{\rm CR}}{\partial z} - \Gamma I. \tag{2}$$

Here $C_{\rm A}$ is the Alfvén velocity, and the time derivative is taken along the characteristics of unstable Alfvén waves, forward propagating with respect to the flow of speed U:

$$\frac{d}{dt} = \frac{\partial}{\partial t} + (U + C_{\rm A})\frac{\partial}{\partial z} \tag{3}$$

Eq.(1) above is essentially a well-known convection-diffusion equation, written for the dimensionless CR partial pressure $P_{\rm CR}$ instead of their distribution function $f(p,t)$. We normalized it to the magnetic energy density $\rho C_{\rm A}^2/2$:

$$P_{\rm CR} = \frac{4\pi}{3}\frac{2}{\rho C_{\rm A}^2} v p^4 f, \tag{4}$$

where v and p are the CR speed and momentum, and ρ- the plasma density. The total CR pressure is normalized to $d\ln p$, similarly to the wave energy density I:

$$\frac{\left\langle \delta B^2 \right\rangle}{8\pi} = \frac{B_0^2}{8\pi}\int I(k)\, d\ln k = \frac{B_0^2}{8\pi}\int I(p)\, d\ln p$$

Eq.(2) is a wave kinetic equation in which the energy transferred to the waves is simply the difference between the total work done by the particles, $(U + C_{\rm A})\nabla P_{\rm CR}$, and the work done on the fluid, $U\nabla P_{\rm CR}$ (Drury 1983). This interpretation of the wave generation indicates that it operates in a maximum efficiency regime. A formal quasilinear derivation of this equation assumes that the particle momentum p is related to the wave number k by the 'sharpened' resonance condition $kp = eB_0/c$ instead of the conventional cyclotron resonance condition $kp_{\|} = eB_0/c$ (Skilling 1975), (note that here $k = k_{\|}$). We have included only the linear wave damping Γ and we will return to the possible role of nonlinear saturation effects later. We assume that $\partial P_{\rm CR}/\partial z \leq 0$ at all times, so that only the forward propagating waves are unstable. The latter inequality is ensured by the formulation of initial value problem in each of the following two settings mentioned earlier in this section. In the first setting, the initial distribution of the CRC is symmetric with respect to $z = 0$, so we can consider their escape into the half-space $z > 0$. The second setting is when the cloud is limited from the left by a reflecting wall (CD). The appropriate boundary condition is $\partial P_{\rm CR}/\partial z = 0$ at $z = 0$ in both cases.

Restricting our consideration to the case of coordinate-independent damping rate Γ, we obtain the following ('quasilinear') integral of the system of Equations (1) and (2):

$$P_{\rm CR}(z,t) = P_{\rm CR0}\left(z'\right) - \frac{\kappa_{\rm B}}{C_{\rm A}}\frac{\partial}{\partial z}\ln\frac{I(z,t)}{I_0(z')} \tag{5}$$

Here $P_{\rm CR0}(z)$ and $I_0(z)$ are the initial distributions of the CR partial pressure and the wave energy density, respectively, and $z' = z - (U + C_{\rm A})t$.

Using the quasi-linear integral, the system of Equations (1) and (2) can be reduced to one nonlinear convection-diffusion equation for e.g., wave intensity $I(z,t)$. We will use dimensionless variables measuring the distance z in units of a, which is the initial size of the CRC. The time unit is then $a/C_{\rm A}$. Note, however, that, as the acceleration is assumed to be inactive, the particle momentum p enters the problem only as a parameter but, the initial scale-height of the CRC a generally depends on p. It is also convenient to introduce a new variable for the wave energy density

$$W = \frac{C_{\rm A} a(p)}{\kappa_{\rm B}(p)} I \tag{6}$$

and similar relations for I_0 and W_0. The equation for W then takes the following form

$$\frac{\partial W}{\partial t} - \frac{\partial}{\partial z}\frac{1}{W}\frac{\partial W}{\partial z} = -\frac{\partial}{\partial z}\mathscr{P}_0(z) \tag{7}$$

We have neglected the wave propagation along the characteristics given by eq.(3) and the wave damping, assuming that these processes are slower than the CRC diffusion: $U, C_{\rm A}, a\Gamma \ll \kappa_{\rm B}/aI \sim cr_{\rm g}/aI$. The function $\mathscr{P}$ is defined similarly to W above

$$\mathscr{P} = \frac{C_{\rm A} a}{\kappa_{\rm B}(p)} P_{\rm CR} \tag{8}$$

and, again, the index 0 refers in Equation (7) to the initial CR distribution $P_{\rm CR0}(z)$. Thus, according to eq.(5), for the dimensionless CR partial pressure we have

$$\mathscr{P} = \mathscr{P}_0 - \frac{\partial}{\partial z} \ln \frac{W}{W_0} \tag{9}$$

This quantity is governed by the equation

$$\frac{\partial \mathscr{P}}{\partial t} = \frac{\partial}{\partial z} \frac{1}{W} \frac{\partial \mathscr{P}}{\partial z}, \tag{10}$$

but its solution can be written down using the integral given by equation (9), after the solution to Equation (7) is obtained.

While letting $C_{\rm A} \to 0$ in the wave-particle collective propagation, we utilize the finiteness of $C_{\rm A}$ in determining the boundary condition for eq.(7) at $z = 0$ as follows. Returning from the nonlinear diffusion equation eq.(7) to eq.(2), one may see that the wave energy does not actually "diffuse" but it is generated locally by particles that diffuse. Therefore, even if the neglected wave diffusion had spread the waves to the point of their stability viz. $z = 0$, they would be convected away from it by virtue of $C_{\rm A} > 0$. Recalling the symmetry (reflection) boundary condition $\partial P_{\rm CR}/\partial z = 0$ at $z = 0$, we must set a fixed boundary value $W(0,t) = W_0$, where W_0 is an initial (small) wave noise. It is instructive to investigate the case in which the initial noise is the same throughout the entire half-space $z > 0$ (this limitation can be straightforwardly relaxed), so that the waves will be generated entirely by escaping particles, thus emphasizing the self-confinement. The second boundary condition is set by $W \to W_0$ for $z \to \infty$, and all $t < \infty$. Note that in general, $W_0 = W_0(p)$. These conditions determine the boundary value problem given by eq.(7) completely. However, we are interested primarily in diffusion of CRs outside the region of their initial localization, viz. at $z > 1$, where the source term in this equation vanishes. Therefore, the problem given by eq.(7) can be split into two separate problems, one in $0 \le z \le 1$ and another in $1 < z < \infty$ domain with the following junction conditions

$$\frac{\partial}{\partial z} \ln W \Big|_{1-}^{1+} = W \Big|_{1-}^{1+} = 0. \tag{11}$$

These are the continuity conditions for both the wave energy density and pressure across the edge of the initial CR localization.

2.2. Self-similar solution outside the region of initial CR localization

The nonlinear boundary value problem in the region $z > 1$ given by Equations (7) and (11) describes the CR propagation outside the region of their initial localization. This problem can be solved exactly using the following self-similar substitution:

$$W = \frac{1}{t^{\alpha}} w(\zeta), \quad \text{where } \zeta = \frac{z}{t^{\beta}} \tag{12}$$

Submitting this to eq.(7) with $\mathscr{P}_0 = 0$ yields $\alpha = 2\beta - 1$. The boundary condition at infinity ($W \to W_0 \neq 0$, $z \to \infty$), on the other hand, requires $\alpha = 0$, so that the equation for w reads

$$\frac{d}{d\zeta}\frac{1}{w}\frac{dw}{d\zeta} + \frac{\zeta}{2}\frac{dw}{d\zeta} = 0 \tag{13}$$

with $\zeta = z/\sqrt{t}$. It is interesting to observe that this equation has a simple special solution $w = 2/\zeta^2 = 2t/z^2$. This solution describes a stationary particle distribution $\mathscr{P} \propto 1/z$ that is obviously related to the Bell (1978) asymptotic particle distribution in self-excited waves far away from a shock. In both cases, this is a singular limit of the problem as it implies a zero background turbulence level, $W_0 = 0$ and thus the number of particles in $z > 0$ half-space being infinite Lagage and Cesarsky (1983); Drury (1983). Physically, this solution is different from what we will find below in that it requires a permanent source of CR at the origin so that their flux steadily drives waves that linearly grow in time.[2] As we shall see, this simple special solution is an important singular limit of a more general and completely regular solution.

The general solution to eq.(13) can be found in quadratures by swapping ζ and w as dependent and independent variables and introducing an auxiliary function $V(w)$ by the following substitution

$$\frac{dw}{d\zeta} = -\sqrt{2} w^{3/2} V(w). \tag{14}$$

The equation for $V(w)$ takes the following form

$$w\frac{d}{dw} w \frac{dV}{dw} + \frac{1}{4}\left(\frac{1}{V} - V\right) = 0 \tag{15}$$

This equation can be easily integrated, so that the function $w(\zeta)$ can be subsequently found from eq.(14). The first integral of eq.(15) is as follows

$$\left(\frac{\partial V}{\partial \ln w}\right)^2 = R(V) \equiv \frac{1}{4}\left(V^2 - 2\ln V - q\right) \tag{16}$$

where q is an integration constant. From eq.(14) and from the boundary condition $w \to W_0$ at $\zeta \to \infty$ we infer that $V(W_0) = 0$, so that from eq.(16) we find

[2]There is no convection with the flow towards the origin ($U = 0$) in our case, which makes the solution unsteady, in contrast to the corresponding DSA problem (Bell 1978) where the solution is steady because of the convection, but the number of particles upstream is still infinite in both cases.

$$w = W_0 e^{\int_0^V \frac{dV'}{\sqrt{R(V')}}} \tag{17}$$

The function $w(\zeta)$ is then determined by the following relation for $\zeta(V)$, eq.(14):

$$\zeta = -\frac{1}{\sqrt{2W_0}} \int \frac{dV}{V\sqrt{R(V)}} e^{-\frac{1}{2}\int_0^V \frac{dV'}{\sqrt{R(V')}}} \tag{18}$$

Using the identity $1/V = V - 2dR/dV$ and integrating eq.(18) by parts, after simple manipulations the last equation rewrites as follows

$$\zeta = \sqrt{\frac{2}{w}} \left(2\sqrt{R} + V\right) \tag{19}$$

It is useful to introduce an auxiliary constant V_1 related to the constant q and being the smaller of the two roots of $R(V)$, that is $R(V_1) = 0$. The requirement of a real zero of the function $R(V)$ ensures mapping two 'copies' of the domain of V onto the full range $0 < \zeta < \infty$, whereby $\zeta \to \infty$ for $V \to 0$. Indeed, $\zeta(V)$ in eq.(19) diverges at $V = 0$ as $\sim \sqrt{-\ln V}$. However, increasing V from $V = 0$ to $V = V_1$ does not cover the full range $0 < \zeta < \infty$ yet, as may be seen from eq.(19); ζ decreases from ∞ only to $\zeta_1 \equiv V_1\sqrt{2/w(V_1)} > 0$. To continue the integral curve to $\zeta = 0$, it is necessary to switch branches of $\sqrt{R}$ at $V = V_1$ in eqs.(17) and (19) and so continue the integral in eq.(17) back to $V < V_1$ (along the second copy of the V-domain). Decreasing then V from $V = V_1$ to $V = V_0 \equiv \exp(-q/2)$ brings the integral curve to the point $\zeta = 0$, $w = w_{\max} = w(\zeta = 0)$. The explicit formal representation of the general solution of eq.(13) is given in Appendix A along with a numerical example. Equations (17) and (19) determine the solution $w(\zeta)$, where the integration constant V_0 (or q) should be obtained from the matching condition, eq.(11). This can be done by considering eq.(7) inside the region of initial CR localization, i.e. $0 < z < 1$, where its r.h.s is nonzero.

2.3. Solution inside the initial CR cloud

Given an initial distribution $\mathscr{P}_0(z)$, equation (7) can always be integrated numerically in the finite domain $0 < z < 1$, so that the full solution will be obtained from the boundary conditions and from the results of the previous section. However, according to Equation (10), already for $t \gtrsim W_0$, where $W_0 \ll 1$, the initial profile $\mathscr{P}_0(z)$ will be redistributed over the unity interval in such a way as to approach a quasi-steady state in which the flux $W_0^{-1}\partial W/\partial z$ in Equation (7) through $z = 0$ will be balanced by the source integral, $\mathscr{P}_0(0)$ (recall that $\mathscr{P}_0(1) = 0$). The particle flux through the $z = 1$ boundary decays as $t^{-1/2}$ with time (since $|\partial w/\partial\zeta| < \infty$ at $\zeta \to 0+$, see the preceding section or Equation (23) below). Therefore, for the self-similar stage of the cloud relaxation we can write

$$\ln\frac{W}{W_0} = \int_0^z \mathscr{P}_0 dz - B(t)\, z \tag{20}$$

where the "integration constant" B depends slowly (in the above sense) on time. Using the first matching condition in Equation (11), i.e., the CR pressure continuity, we can specify $B(t)$ as follows: $B \propto t^{-1/2} \to 0$

as $t \to \infty$ (see Equation [23] below). This determines the self-similar (outer, $z > 1$) solution by the second matching condition in Equation (11):

$$w(0) \equiv \lim_{t\to\infty} w\left(\frac{1}{\sqrt{t}}\right) = w_{\max} = W_0 e^{\Pi} \tag{21}$$

Here we have introduced the integrated partial pressure as follows

$$\Pi = \int_0^1 \mathscr{P}_0 dz. \tag{22}$$

The function $B(t)$ and thus the internal solution $W(z,t)$ in Equation (20) may be obtained using this equation, the first matching condition in Equation (11), and Equations (14)

$$B(t) = -\frac{1}{\sqrt{t}}\frac{\partial}{\partial\zeta}\ln w\Big|_{\zeta=1/\sqrt{t}} = \sqrt{2w/t}V\Big|_{\zeta=1/\sqrt{t}} \tag{23}$$

Note that the particle pressure at $z > 1$ is completely determined by the turbulence level w, eq.(9).

Now we can determine the integration constant q introduced in the preceding section. From Equations (21) and (A3) we obtain the following equation for q

$$\int_0^{V_1} dV/\sqrt{R(V)} + \int_{V_0}^{V_1} dV/\sqrt{R(V)} = \Pi, \tag{24}$$

where $R(V_1) = 0$, $R(V_0) = -V_0/2$, while $R(V)$ is given by Equation (16). In the most interesting case $q \approx 1$, it is convenient to use the constant $\varepsilon^2 = (q-1)/2$ in place of q. In this case $\Pi \gg 1$, $\varepsilon \ll 1$, $V_1 \approx 1-\varepsilon$ and

$$\Pi = 2\int_0^{V_1} \frac{dV}{\sqrt{R}} \approx 2^{3/2}\int_0^{1-\varepsilon} \frac{dV}{\sqrt{(V-1)^2-\varepsilon^2}} \approx 2^{3/2}\ln\frac{2}{\varepsilon} + \mathscr{O}(1),$$

so that the turning point of the solution at $V = V_1$ approaches the critical point $V = 1$, where R has a minimum (Fig.2):

$$V_1 = 1 - 2e^{-\Pi/2\sqrt{2}}.$$

For $\Pi \ll 1$, we can write instead, $V_1 \approx V_0\left(1 + V_0^2/2\right)$ where $V_0 = \exp(-q/2)$.

To conclude this section, the self-similar expansion of the CRC described by Equations (7-10) is controlled by two parameters. One parameter is the background turbulence level $W_0(p)$ in the media into which the cloud expands. The second parameter is the integrated pressure of the cloud, Π. Although the initial wave energy density inside the cloud ($z < 1$) is likely to be higher than W_0, we have adopted the background value W_0 also inside the cloud for simplicity, as it should not influence the self-similar CR propagation outside the cloud. In addition, efficent wave generation by a dense expanding CRC, renders the initial value for the wave energy density inside the CRC unimportant.

3. Analysis of the solution

Once we have the solutions outside and inside the region of initial CR localization, we may precisely calculate how fast particles escape from this region. Two convenient characteristics of the escape process are the half-life time and the width of the CR distribution. We begin our analysis of the solution from computing these simple quantities and turn to the details of the CR escape afterwards.

3.1. Half-life time and the width of the CR cloud

The most concise characterization of the escape may be given by looking at the following two parts of the (conserved) integral particle pressure:

$$\Pi = \Pi_0 + \Pi_1 = \text{const}$$

where

$$\Pi_0 = \int_0^1 \mathscr{P} dz \quad \text{and} \quad \Pi_1 = \int_1^\infty \mathscr{P} dz$$

refer to the regions inside and outside of the initial CRC, respectively. Recall that at $t = 0$, $\Pi_0 = \Pi$ and $\Pi_1 = 0$, while at $t = \infty$, an opposite CR distribution is reached: $\Pi_0 = 0$ and $\Pi_1 = \Pi$. Note that Equation (21) specifies the total work ultimately done by particles on waves, while they diffuse from $0 < z < 1$ to $1 \leq z < \infty$. As Π is conserved, it is natural to define the CR confinement time as the time at which Π_0 (Π_1) drops (raises) to a half of Π. Substituting W from Equation (12) into Equation (9), we obtain

$$\Pi_1(t) = \ln \frac{w}{W_0}\bigg|_{\zeta = 1/\sqrt{t}}$$

For the half-life time $t = t_{1/2}$ we may use the following equations:

$$\Pi_1\left(t_{1/2}\right) = \Pi_0\left(t_{1/2}\right) = \frac{1}{2}\Pi. \tag{25}$$

In the simple test particle case ($\Pi \ll 1$), the half-life amounts to (see Appendix B)

$$t_{1/2} \approx \frac{1}{4\sigma} W_0 \tag{26}$$

with $\sigma \approx 0.48$. In the opposite case $\Pi \gg 1$, for $t_{1/2}$ we obtain

$$t_{1/2} \approx t_1 = 1/\zeta_1^2 \equiv \frac{w_1}{2V_1^2} \approx \frac{w_1}{2} \tag{27}$$

(see Equation [19]). Note that for $\Pi \gg 1$, $V_1 \approx V_{1/2}$, (see Appendix B) and for the half-life time we obtain

$$t_{1/2} = \frac{1}{2} W_0 e^{\Pi/2} \tag{28}$$

We may extend the last formula with a 5 percent accuracy also to the linear case ($\Pi \ll 1$), given by Equation (26). It is clear that the nonlinear delay factor $\exp(\Pi/2)$ slows down the escape considerably, compared to the test particle solution.

Another important characteristics of the particle escape is the spatial width of their distribution. Formally, the self-similar solution is scale-invariant $\sim 2/\zeta$, for $\Pi \gg 1$ over the most part of the spatial distribution of the partial pressure (see below). Therefore, to characterize the width we use the point $\zeta_{1/2}$, related to the half time $t_{1/2}$ as follows:

$$\zeta_{1/2} = \frac{1}{\sqrt{t_{1/2}}} = \sqrt{\frac{2}{W_0}} e^{-\Pi/4}$$

In physical coordinate z, this point moves outwards as $z_{1/2} = \zeta_{1/2}\sqrt{t}$ starting from $z = 1$ at $t = t_{1/2}$. The expansion rate of a dense CRC ($\Pi \gg 1$) is thus exponentially low.

3.2. Spatial distribution of the CR cloud

Considering the spatial distribution of the spreading CRC in detail, it is convenient to start with the region far away from the source, where $W \to W_0$. This asymptotic behavior corresponds to the case $V \ll 1$. Introducing an auxiliary function $U(\zeta)$

$$U = -\frac{\partial}{\partial \zeta} \ln w = \sqrt{2w} V \tag{29}$$

that is related to the particle pressure through $\mathscr{P} = U(\zeta)/\sqrt{t}$, and using Equations (16) and (19), we obtain for U the following expression

$$U(\zeta) = \sqrt{2W_0} V_0 e^{-W_0 \zeta^2/4} \tag{30}$$

Therefore, the asymptotic CR pressure depends on the following two parameters: the ISM background diffusivity $W_0^{-1}(p) \equiv W^{-1}(p, z = \infty)$ (see Equation [10]) and on the CR source pressure $\Pi(p)$, but only through the parameter $V_0 = \exp(-q/2)$. The latter grows linearly with $\Pi \ll 1$ but it saturates when $\Pi \gg 1$:

$$V_0 \approx \begin{cases} \frac{1}{\sqrt{2\pi}}\Pi, & \Pi \ll 1 \\ \exp\left(-\frac{1}{2} - 4e^{-\Pi/\sqrt{2}}\right), & \Pi \gg 1 \end{cases} \tag{31}$$

For practical calculations, it is more convenient to combine both asymptotic regimes into the following simple interpolation formula:

$$V_0 = \left[\left(\sqrt{2\pi}/\Pi\right)^{5/2} + \left(\sqrt{e} + \frac{3}{2} e^{-\Pi/\sqrt{2}}\right)^{5/2} \right]^{-2/5} \tag{32}$$

which not only recovers both $\Pi \ll 1$ and $\Pi \gg 1$ regimes but also reproduces the transition zone accurately. The latter property is achieved by the choice of numerical parameters of the interpolation, i.e., $5/2$, $3/2$ and $2/5$. The quality of the interpolation may be seen from Fig.4, where the formula in Equation (32) is shown against exact numerical points calculated from Equation (24). The partial pressure $\mathscr{P}(z,t)$ is then given by

$$\mathscr{P} = U/\sqrt{t} = \sqrt{2W_0/t}V_0(\Pi)\, e^{-W_0 z^2/4t} \tag{33}$$

Note, that for strong sources ($\Pi \gg 1$) the CR density at large distances becomes independent of the source strength. This is the regime of an efficient ablative escape reduction in which a small (and Π-independent!) number of leaking particles leave behind enough Alfvén fluctuations to limit the leakage of particles remaining in the source to exactly the rate given by Equation (33).

The spatial distribution of the CRs becomes even more universal closer to the origin where it falls off as $\mathscr{P} \approx 2/z$ before it turns into an innermost flat-top part of the entire distribution for $\zeta^2 < D_{\rm NL}(p)$. We have introduced the "self-confinement" diffusion coefficient $D_{\rm NL}$ as

$$D_{\rm NL} = \frac{2}{V_0^2} D_{\rm ISM} e^{-\Pi} = \frac{2}{V_0^2 w_{\max}} \tag{34}$$

with $D_{\rm ISM} = W_0^{-1}$. To obtain this intermediate ($D_{\rm NL} < \zeta^2 < D_{\rm ISM}$) part of the CR spatial distribution we expand the analytic solution given by Equations (17) and (19) in small $V_1 - V \ll 1$. Using the expression for the self-similar CR pressure U from Equation (29) we obtain for this quantity the following expansion near $\zeta = \zeta_1 \equiv \zeta(V_1)$:

$$U = \frac{2}{\zeta}\left[1 - \left(1+\frac{1}{\sqrt{2}}\right)\left(\frac{2}{w_1}\right)^{1/\sqrt{2}} \frac{\varepsilon}{\zeta^{\sqrt{2}}} + \ldots\right], \tag{35}$$

where $w_1 = 2V_1^2/\zeta_1^2$. Note that while the solution has a branching point in auxiliary variable V at $V = V_1$, it is regular and single-valued function of the physical variable ζ, throughout the entire half space $\zeta > 0$, including the branching point of $\zeta(V)$ at $V = V_1$, as it should be. We also notice that while ζ decreases starting from ζ_1, the solution grows slower than $1/\zeta$, leveling off towards the origin. The above expansion, however, becomes inaccurate for smaller ζ and we alter it below.

Now we turn to this innermost part of the distribution where the particle diffusion coefficient is most strongly decreased. It is convenient to expand the solution in a series in $\xi = V/V_0 - 1 \ll 1$. Using the representation of w given by Equation (A2), we obtain

$$w = w_{\max}\left[\frac{\xi - a + \sqrt{\xi^2 - 2a\xi + b^2}}{b-a}\right]^{-2b}$$

where $a = \left(1-V_0^2\right)/\left(1+V_0^2\right)$ and $b = V_0/\sqrt{1+V_0^2}$. Then, using the expression (A4) for small ζ and Equation (29), we obtain for $U(\zeta) = \mathscr{P}\sqrt{t}$ the following simple result

$$U = \frac{\sqrt{2w_{\max}}V_0}{1 + w_{\max}\zeta^2/4}, \tag{36}$$

valid for $w_{\max}\zeta^2 \lesssim 1$. Note that, with the same accuracy, the denominator can be recast in the standard "diffusion" form, $\exp\left(w_{\max}\zeta^2/4\right)$, in which the CR diffusivity is diminished by a factor $W_0/w_{\max} = \exp(-\Pi) \ll 1$ compared to its background level. If, however, $w_{\max} \gtrsim aC_{\rm A}/\kappa_{\rm B}$ (see Equation [6]), a better approximation would be to simply replace the diffusion coefficient by its Bohm value, as the neglected nonlinear wave interactions (see Sec.4) should render $\delta B \sim B_0$. The result in Equation (36) should then be replaced by

$$U = \sqrt{2aC_{\rm A}/\kappa_{\rm B}}V_0(\Pi)\, e^{-aC_{\rm A}z^2/4\kappa_{\rm B}t} \tag{37}$$

The overall distribution of $U(\zeta) = \mathscr{P}\sqrt{t}$ is well reproduced by the following parametrization, Fig.5

$$U = 2\left[\zeta^{5/3} + (D_{\rm NL})^{5/6}\right]^{-3/5} e^{-W_0\zeta^2/4} \tag{38}$$

where $V_0(\Pi)$is given by the interpolation in Equation (32). The last formula recovers the limiting cases given by Equations (30), (35) and (36) except a slight modification of Equation (30) at large ζ , so that an extra $1/\zeta$-factor is accepted in the interests of the simplicity of the parametrization. According to Fig.5, however, this deviation from the correct asymptotic expansion of the exponential tail of the distribution is not really noticeable.

The overall profile of the partial pressure (Fig.5) unveils the CR escape as a highly structured process. It comprises a nearly flat-top core, a $1/\zeta$ pedestal and an exponential foot. We already noted that the escape rate of CR in the foot saturates with the source strength for $\Pi \gg 1$. This is easy to understand as the foot is separated from the core (source) by the pedestal, where the CR transport is self-regulated so that a fixed CR flux streams through it to the foot. The solution is shown in Fig.5 as a function of ζ using the self-similar variables $U = \mathscr{P}\sqrt{t}$ and $\zeta = z/\sqrt{t}$. Remarkably, the pedestal portion of the profile does not change with time also in the physical variables, $\mathscr{P}, z$: $\mathscr{P} \approx 2/z$. The core, however, sinks in as $\mathscr{P} \propto 1/\sqrt{t}$ but in addition, it expands in z as $\sqrt{D_{\rm NL}t}$, to conserve the integrated pressure contained in the core at the expense of the pedestal that shrinks accordingly. The latter disappears completely at $t \sim D_{\rm ISM}/D_{\rm NL}$, after which the further escape proceeds in a test particle regime but with a smaller diffusion coefficient in the core-pedestal region, since waves persist even after the most of particles have escaped.

As the test particle approximation is widely used in calculating the CR escape from their sources, we also show, for comparison, one such example in Fig.5. We plot the following simple test particle solution

$$U = \sqrt{\frac{W_0}{\pi}}\Pi e^{-W_0\zeta^2/4}$$

that can be obtained from Equation (38) or (33) with $V_0(\Pi)$ taken from Equation (31) or (32) for $\Pi \ll 1$. However, we formally extend this linear result to large Π, as this is normally done within test particle approaches. Such an extension clearly underestimates the nonlinear level of the CR pressure by a factor $\sim \Pi^{-1}\exp(\Pi/2) \gg 1$ in the core and in the most of the pedestal. By virtue of lacking self-regulation, it overestimates the pressure in the exponential foot by a factor $\Pi \gg 1$.

3.3. Control parameters and predicted CR flux in physical units

The integrated partial pressure Π is the most important parameter that regulates the CR escape. Therefore, we consider it in some detail, returning to the dimensionful variables and rewriting Π as follows (see

Equations [8] and [22]):

$$\Pi \simeq 3\frac{C_{\rm A}}{c}\frac{a(p)}{r_{\rm g}(p)}\frac{\bar{P}_{\rm CR}(p)}{B_0^2/8\pi}, \tag{39}$$

where $a(p)$ is the initial size of the CRC, $r_{\rm g}$ is the CR gyroradius and $\bar{P}_{\rm CR}(p)$ is their average partial pressure inside the cloud. Although the ratio of Alfvén speed to speed of light, $C_{\rm A}/c$ is typically very small ($\sim 10^{-5}-10^{-4}$), the remaining two ratios in the last equation may be fairly large. Indeed, $a/r_{\rm g}$ should amount to several $c/U_{\rm EST} \gg 1$, with $U_{\rm EST}$ being the shock speed at the end of the Sedov-Taylor stage, as a scales at least as the precursor size. In fact, a significant part of the shock downstream region filled with CR, that have been convected there over the entire history of CR production, may significantly contribute to, if not dominate, the total length of the cloud a. This is particularly relevant to the CR release during the decreasing maximum energy (reverse acceleration phase) Gabici (2011). In the forward acceleration regime (growing maximum energy) Bohm diffusion, the downstream CR scale height is similar to that of the upstream. A reasonable estimate for $U_{\rm EST}$ is $c/U_{\rm EST} \gtrsim 10^3$. Finally, the CR pressure in the source should considerably exceed the magnetic pressure as both quantities are roughly in equipartition in the background ISM. Alternatively, as is usually assumed, the accelerated electrons are in equipartition with the magnetic energy inside the source, since they should have lost their excessive energy via synchrotron radiation. As electrons are thought to be involved in the acceleration at $\sim 10^{-2}$ of the proton level, the last ratio in Equation (39) is at least $\gtrsim 10^2$, thus raising the pressure parameter to $\Pi \gg 1$.

One of a few other ways the parameter Π can be looked at is to express it through the average acceleration efficiency $\mathscr{E} = 2\bar{P}_{\rm CR}/\rho\bar{U}^2$, where $\bar{U}$ is the shock velocity, appropriately averaged over the CR acceleration history (one may expect $\bar{U} \gg U_{\rm EST}$). Then $\Pi \simeq 3\left(\bar{U}^2/cC_{\rm A}\right)\left(a/r_{\rm g}\right)\mathscr{E} \simeq 3A\left(\bar{U}^2/U_{\rm EST}C_{\rm A}\right)\mathscr{E}$, where we have introduced a factor $A = \left(a/r_{\rm g}\right)U_{\rm EST}/c \gtrsim 1$. In this form, the estimate indeed boils down to the acceleration efficiency $\mathscr{E}$ with the remaining quantities ($A, \bar{U}$ and $U_{\rm EST}$) being more accessible to specific models. Since the acceleration efficiency $\mathscr{E}$ is believed to be at least $\gtrsim 0.1$ for productive SNRs, we conclude that the control parameter Π is rather large than small. The caveat here is that it might, in some cases, be too large to limit the applicability of the above treatment. We return to this issue in the Discussion section.

Once the major control parameter is known, we can calculate the distribution function $f_{\rm CR}$ of the CR, released into the ISM, depending on the distance from the source z and time, using the parametrization in Equation (38). It is convenient to rewrite it in the form of the CR partial pressure $\hat{P}_{\rm CR}$ in physical units as follows

$$\frac{\hat{P}_{\rm CR}}{B_0^2/8\pi} \simeq 0.8\left(\frac{M_{\rm A}}{A}\frac{10^4{\rm yrs}}{t}\frac{n}{1{\rm cm}^{-3}}\frac{E}{1{\rm GeV}}\right)^{1/2}\left(\frac{1\mu{\rm G}}{B}\right)^{3/2}U(\zeta) \tag{40}$$

Here $M_{\rm A} = U_{\rm EST}/C_{\rm A}$, n is the plasma number density, E is the particle energy and B is the magnetic field. The self-similar coordinate ζ can be represented, in turn, in the following way

$$\zeta \simeq 17\left(\frac{M_{\rm A}}{A}\frac{1{\rm GeV}}{E}\frac{B}{1\mu{\rm G}}\frac{10^4{\rm yrs}}{t}\right)^{1/2}\frac{z}{\rm pc} \tag{41}$$

Once this quantity is calculated for given z and t, the CR partial pressure in Equation (40) can be obtained

from Equation 38 or from Fig.5. Note that the scale of the CR pressure is determined by the maximum of $U = U(0) = \sqrt{2W_0}V_0 \exp(\Pi/2)$, where V_0 is given by Equation (32). The CR partial pressure also depends on the energy through W_0 and Π, apart from the factor $\sqrt{E}$ in Equation (40), which will be discussed below. Finally, the background diffusion coefficient of CR in physical units is related to the dimensionless diffusivity W_0^{-1} as follows

$$D_{\rm ISM} = 6.6 \cdot 10^{27} \frac{10^{-4}}{W_0} \frac{a}{1{\rm pc}} \frac{B}{1\mu G} \left(\frac{1{\rm cm}^{-3}}{\rm n}\right)^{1/2} \frac{{\rm cm}^2}{\rm sec}.$$

3.4. The Form of the Spectrum of escaping CR

As the transition from the flat-top part of the normalized (Equation [8]) partial pressure $\mathscr{P}(p)$ to the pedestal is described by a function $\mathscr{P} \approx 2\left\{z^{5/3} + [D_{\rm NL}(p)\,t]^{5/6}\right\}^{-3/5}$, the pressure $\mathscr{P}(p)$ is almost p-independent (the corresponding particle momentum distribution $f_{\rm CR} \propto \kappa_{\rm B} p^{-4}/\hat{z}$, in the physical units, $\hat{z} = az$) for such momenta where $D_{\rm NL}(p) < z^2/t$, for the fixed dimensionless observation point z and time t. At $p = p_{\rm br}$, where $D_{\rm NL}(p_{\rm br}) = z^2/t$, the spectrum incurs a break. If we approximate $D_{\rm NL} \propto p^{\delta}$ near $p \sim p_{\rm br}$, the break will have an index $\delta/2$, as may be seen from the above formula for $\mathscr{P}$. The index δ thus derives from the momentum dependence of the $D_{\rm ISM}(p)$ and from that of the coordinate integrated CR pressure $\Pi(p)$ (through the factor $\exp(-\Pi)$ in equation [34]). Furthermore, if we represent $\exp(-\Pi) \propto p^{-\sigma}$ and $D_{\rm ISM} \propto p^{\lambda}$ at $p \sim p_{\rm br}$, so that $\delta = \lambda - \sigma$, then $\mathscr{P}$ is flat at $p < p_{\rm br}$ for $\delta > 0$ and steepens to $p^{-\delta/2}$ at $p = p_{\rm br}$. Conversely, if $\delta < 0$, $\mathscr{P}$ raises with p as $p^{-\delta/2}$ at $p < p_{\rm br}$ and it levels off at $p > p_{\rm br}$. Note, however, that Π is momentum independent in the important case of the p^{-4} distribution of the initial CRC with the scale height $a(p) \propto \kappa_{\rm B}$. This case corresponds to the test-particle DSA spectrum, $\propto p^{-4}$ with a scale height a estimated from the shock precursor size. The break has then an index $\lambda/2$ and it is entirely due to the $D_{\rm ISM}$ momentum dependence.

4. Comparison with other approaches

Given a number of different approaches to the CR escape, we extend our brief discussion in the Introduction to compare them with the above-developed treatment. Most of the approaches can be categorized into the following three kinds. First of all, a simple test particle approach (TP) is feasible for a rarefied CRC, when wave generation is negligible (e.g., Aharonian and Atoyan 1996; Drury 2011; Ohira *et al.* 2011). It solves the *linear* diffusion equation for the CRs with a diffusion coefficient determined by a given (e.g., background) turbulence. Next, there are extensions that also estimate the wave generation by escaping particles and determine the nonlinearly saturated waves, mostly by considering MHD cascades (e.g., Ptuskin and Zirakashvili 2005; Ptuskin *et al.* 2008; Yan *et al.* 2012). The wave intensity, thus obtained, is then used to calculate the particle diffusion coefficient and their distribution. We tentatively call these approaches modified test particle, as they still do not treat particles and waves on an equal footing. By the conventional plasma physics methodology this improvement of the TP models overjumps the quasi-linear (QL) treatment, where wave stabilization occurs through their backreaction on the particles (suppression of instability by pitch-angle isotropization) and not through the nonlinear saturation. As this is the lowest

order process in the wave energy that limits the wave growth, it is imperative to consider it first. We thus pursue a conventional plasma physics approach, similar to a classical problem of expansion of a hot electron cloud into a plasma (Ryutov and Sagdeev 1970; Ivanov *et al.* 1970). As we also noted earlier, there is an extended region (i.e. "pedestal" self-confinement region) where the level of turbulence strongly exceeds its background value but is stilll not high enough for the nonlinear effects to dominate over the quasilinear ones. As our results show, this is dynamically the most important domain that determines the spectrum of escaping CRs. Simply put, the dynamics is dominated by wave generation and self-regulated particle escape, rendering the nonlinear wave dynamics and MHD cascades less important. It should be noted, however, that the instability driving pitch-angle anisotropy is supported by the spatial inhomogeneity of the CRC, so that the full stabilization occurs (under negligible damping) only when particles spread to infinity.

The above-described approaches to the CR escape are charted in Fig.6. The key ingredients are the CR particles and Alfven waves while the relevant physical phenomena are the wave-particle and wave-wave interactions. Under the latter we loosely understand both weakly-turbulent parametric processes (such as wave decay) and turbulent cascades. The wave-particle interactions comprise the unstable growth of Alfven waves together with their back-reaction on the CRs. Wave-wave interactions need to be included in the quasi-linear treatment, particularly in the core of the CRC when $w_{\max} \gtrsim 1$, but the exact analytic solution obtained in this paper will hardly be possible to extend to the fully nonlinear treatment. Therefore, at present we may employ the Bohm diffusion coefficient in this region, i.e. where $z^2/t \lesssim D_{\rm NL}$ by setting $D_{\rm NL} \sim \kappa_{\rm B}$ and thus obtain the expression in Equation (37), which formally amounts to the test-particle result with the diffusion coefficient decreased to its minimum, i.e. Bohm value.

To summarize our results, we have considered the self-consistent relaxation of a CR cloud (CRC) injected into a magnetized plasma (ISM) under the assumption of an initially weak background turbulence, $(\delta B/B_0)^2 \ll 1$, so that the cross-field diffusion is negligible, $\kappa_\perp \ll \kappa_\parallel$ *outside* the cloud and the particles escape largely along the field, i.e., in z-direction. The principal parameter that regulates the CR escape from the cloud is identified to be their coordinate-integrated partial pressure Π, given e.g., in Equation (39). Resonant waves of the length $\sim r_{\rm g}^{-1}(p)$, driven by the run-away cloud particles, are found to confine the core CRs very efficiently when $\Pi \gg 1$.

The resulting normalized (Equation [8]) CR partial pressure profile $\mathscr{P}$ comprises the following three zones: (i) a quasi-plateau (core) at small $z/\sqrt{t} < \sqrt{D_{\rm NL}}$ of a height $\sim (D_{\rm NL}t)^{-1/2}$, which is elevated by a factor $\sim \Pi^{-1}\exp(\Pi/2) \gg 1$, compared to the test particle solution because of the strong quasi-linear suppression of the CR diffusion coefficient with respect to its background (test particle) value $D_{\rm ISM}$: $D_{\rm NL} \sim D_{\rm ISM}\exp(-\Pi)$ (ii) next to the core, where $\sqrt{D_{\rm NL}} < z/\sqrt{t} < \sqrt{D_{\rm ISM}}$, the profile is scale invariant, $\mathscr{P} \approx 2/z$. The CR distribution in this "pedestal" region is fully self-regulated, independent of Π and $D_{\rm ISM}$ for $\Pi \gg 1$, (iii) the tail of the distribution at $z/\sqrt{t} > \sqrt{D_{\rm ISM}}$ is similar in shape to the test particle solution but it saturates with $\Pi \gg 1$, so that the CR partial pressure is $\propto (D_{\rm ISM}t)^{-1/2}\exp\left(-z^2/4D_{\rm ISM}t\right)$, independent of the strength of the CR source Π, in contrast to the test-particle result that scales as $\propto \Pi$. Because of the CR diffusivity reduction, the CRC half-life is increased and the cloud width is decreased, compared to the test particle solution.

Depending on the functions $\Pi(p)$ and $D_{\rm ISM}(p)$, the resulting CR spectrum generally develops a spectral break for the fixed values of z and t such that $z^2/t \sim D_{\rm NL}(p) \sim D_{\rm ISM}\exp(-\Pi)$.

5. Discussion and Outlook

The CR escape from both active and fading accelerators (old SNR) is being actively studied through direct observations of CR illuminated molecular clouds (Aharonian *et al.* 2008; Abdo *et al.* 2010c,a; Giuliani *et al.* 2011; Aleksić *et al.* 2012; Uchiyama *et al.* 2012). To date, most of the information is obtained from the old remnants and they consistently show a broad spectrum CR escape. This is clearly at odds with an intuitive high energy biased escape, seemingly justified by the higher mobility of energetic CRs. Indeed, as CR diffusion coefficient grows with momentum, the test-particle solution predicts a low-energy cutoff to be present due to the factor $\exp\left[-z^2/4D_{\rm ISM}(p)t\right]$ in the CR distribution at a certain distance from the source. In a combination with a steep power-law or a favorably placed upper cutoff, the escape flux narrowly accumulates towards the maximum energy. The momentum dependent CR mobility underlies most of the current CR escape models (e.g., Ptuskin and Zirakashvili 2005; Zirakashvili and Ptuskin 2008; Gabici *et al.* 2009).

Although the same exponential factor is present in the QL solution obtained in this paper, it pertains only to the farthermost zone, where the CR partial pressure is much lower (by factor $\Pi^{-1} \ll 1$) than the test particle prediction for the same distance from the source and time elapsed from the CR release. Closer to the accelerator, in an extended scale-invariant zone where the CR level is much higher and decays as slowly as $1/z$, the escape mechanism is different from the one controlled by the mere energy dependence of the CR diffusivity. It is self-regulated in such a way that, if particles leak excessively in some energy range, they also drive stronger resonant waves to reduce their leakage and vice versa. As a result, the overall escape spectrum relaxes roughly to an equipartition of the CR partial pressure in momentum, e.g., $f_{\rm CR} \propto p^{-4}$ (with important deviations described in Sec.3.4), which also balances the driver (gradient of CR partial pressure) with the generated waves. No low-energy leakage suppression therefore occurs. The fundamental difference of this leakage mechanism from the test particle one is that it is entirely controlled by self-generated rather than prescribed waves, or by waves derived from other energy sources, such as ambient MHD cascades. That is why it predicts energetically much broader leakage than many other approaches do (e.g., Ptuskin and Zirakashvili 2005; Ellison and Bykov 2011)

It should be admitted that the self-confinement solution obtained in this paper is strictly valid for a stopped accelerator, so that there is no CR energy growth and associated strong plasma flows, such as those found near shocks. Therefore, care should be exercised in comparing this solution with the standard DSA predictions. Nevertheless, particles that escape from the DSA through free escape boundary (FEB) or the upper momentum cutoff, are likely to propagate further out diffusively. Their escape is, in fact, enforced by imposing an ad hoc sudden jump in the diffusion coefficient at a specific momentum (or FEB position) that advances in time according to the acceleration rate and shock evolution. Despite this jump, the CR phase space density just at the cutoff (or FEB) must be continuous,[3] i.e., still high enough to drive waves while the CR escape. From this point on, the solution obtained in this paper may be applied and compared with the DSA predictions, as the waves are driven locally both in momentum and in coordinate space, and the only relevant requirement is that particles do not interact with the shock, as implied in most escape models in the first place. But, the feedback from the self-generated waves on the CR escape is not included in the models

[3]This statement is strictly valid for a FEB imposed by enhanced diffusion in coordinate space. In the case of a jump in momentum (e.g., Ptuskin and Zirakashvili 2005), the situation is more complicated in that the particle distribution should become increasingly anisotropic in pitch angle, as the escape is assumed one-sided (upstream). However, an introduction of weak Fermi-II acceleration (diffusion in momentum) would validate this statement also in this case.

that predict a peaked energy escape.

Furthermore, the self-regulated escape solution shows a gradual increase of the CR diffusion from a low (Bohm) to high (TP) regime, and most of this growth occurs where the solution is scale-invariant, i.e. the partial pressure $\mathscr{P} \propto 1/z$ and the CR diffusion coefficient $D_{\rm NL} \propto z^2$, thus keeping the flux across the scale invariant (pedestal) region $-D_{\rm NL}\nabla\mathscr{P} \approx$ const. Both scalings are clearly inconsistent with a sudden jump in $D_{\rm NL}$ with the corresponding jump in $\nabla\mathscr{P}$. Moreover, collapsing the scale-invariant region to a point would not only change the CR escape flux considerably but, an extended and observationally important region of the enhanced CR pressure would be completely lost (see Fig.5). This region (which we loosely dubbed "pedestal" by analogy with the improved confinement regimes in magnetic fusion devices, primarily in tokamaks e.g., Wagner *et al.* 1982; Hinton and Staebler 1993; Diamond *et al.* 1995; Malkov and Diamond 2008; Maggi 2010) may be detectable when it overlaps with molecular clouds. According to the test-particle theory the CR density decays as $t^{-d/2}$ in the region of their initial release, with d being the dimensionality of the escape ($d = 1$ for escape along the field). In the self-regulated escape, the CR density stays constant in time in the pedestal region, where $P_{\rm CR} \propto 1/z$, until this region is overwhelmed by the expanding central plateau where $P_{\rm CR}$ decays as $1/\sqrt{t}$. Besides that the CR density is significantly higher there than in the test-particle case, Fig.5, which is the prediction that may soon become testable.

Recent detailed observations of the SNR W44, W51C, IC 443 and W28 surrounded by dense MC provide good examples to study possible CR escape scenarios (Aharonian *et al.* 2008; Abdo *et al.* 2010b,c,a; Giuliani *et al.* 2011; Aleksić *et al.* 2012; Uchiyama *et al.* 2012). First of all they invariably show spectral breaks that, however, may be understood in terms of the interaction of accelerated protons with a partially ionized dense gas (Malkov *et al.* 2005, 2011). The indices below and above the breaks are consistent with the following two scenarios. Namely, CR protons may reach the molecular cloud while still being accelerated at a SNR shock, or they may escape with a similar spectrum, p^{-4}. As we have shown in the present paper, such escape occurs via the CR interaction with self-generated waves. Another important aspect of these observations regards the morphology of the interaction. Of particular interest is the recent analysis of Fermi-LAT results revealing two bright spots of gamma emission adjacent to the central source in W28 (Uchiyama *et al.* 2012). Their distinct bi-polar appearance may be indicative of a CR escape along the local magnetic field.

Note that the anisotropic diffusion of cosmic rays in the form of bipolar CRC may result in quite specific morphologies of extended gamma-ray images - the imprints of cosmic rays interacting with the surrounding diffuse gas are generally concentrated in dense molecular clouds. Since the gamma-ray flux is proportional to the product of densities of CRs and the diffuse gas, we should expect a rather general correlation between the gamma-ray fluxes and the column densities of the interstellar gas. However, it is obvious that in the case of propagation of bipolar CR clouds through an inhomogeneous clumpy gaseous environment, the gamma-ray intensity contours can significantly deviate from the CO and 21cm maps characterizing the spatial distributions of the molecular and atomic gases, respectively. At the same time, the brightest parts of the spatial distribution of gamma-rays should correspond to the regions where the CR cloud overlaps with dense gas clouds inside the magnetic flux tube connected with the CR source.

Support by the Department of Energy, Grant No. DE-FG02-04ER54738 is gratefully acknowledged. P.H.D. acknowledges support from WCI Program of the National Research Foundation of Korea (NRF) (NRF Grant Number: WCI 2009-001).

A. Details of self-similar solution

The full expressions for the solution $w(\zeta)$ represented in a short form by eqs.(17) and (18) can be written as follows

$$w = W_0 \begin{cases} e^{\int_0^V dV/\sqrt{R(V)}}, & \zeta \geq \zeta_1 \\ e^{\int_0^{V_1} dV/\sqrt{R(V)} + \int_V^{V_1} dV/\sqrt{R(V)}}, & 0 < \zeta < \zeta_1 \end{cases} \tag{A1}$$

In some cases, it is convenient to represent w in the domain $0 < \zeta < \zeta_1$ as

$$w = w_{\max} e^{-\int_{V_0}^{V} dV/\sqrt{R(V)}} \tag{A2}$$

where $V_0 \equiv \exp(-q/2)$, i.e., $\zeta(V_0) = 0$, and

$$w_{\max} = W_0 e^{\int_0^{V_1} dV/\sqrt{R(V)} + \int_{V_0}^{V_1} dV/\sqrt{R(V)}}. \tag{A3}$$

For the coordinate ζ we have

$$\zeta = \sqrt{\frac{2}{w}} \begin{cases} V + 2\sqrt{R(V)} & \zeta \geq \zeta_1 \\ V - 2\sqrt{R(V)} & 0 < \zeta < \zeta_1 \end{cases} \tag{A4}$$

Throughout this Appendix, the positive branch of $\sqrt{R}$ is used. The partial CR pressure can be represented according to eq.(9) as follows

$$\mathscr{P}(z,t) = \sqrt{2w(\zeta)/t} V(\zeta)\Big|_{\zeta = z/\sqrt{t}}, \quad z > 1$$

where $V(\zeta)$ is defined by eq.(A4).

B. Half-life of the CR cloud

Equation (25) can be continued as

$$\Pi_1\left(t_{1/2}\right) = \frac{1}{2}\Pi = \frac{1}{2}\ln\frac{w_{\max}}{W_0} \equiv \ln\frac{w_{1/2}}{W_0} \tag{B1}$$

where we have introduced a "half-life" amplitude $w_{1/2}$, which can also be associated with a point $V_{1/2}$ (see Equation[17])

$$\ln\frac{w_{1/2}}{W_0} = \int_0^{V_{1/2}} dV/\sqrt{R(V)},$$

and with the corresponding self-similar coordinate $\zeta_{1/2} = 1/\sqrt{t_{1/2}}$. In other words, $w_{1/2} = w\left(\zeta_{1/2}\right) = w\left(V_{1/2}\right)$. Note that $w_{1/2}$ can be represented as a geometric mean $w_{1/2} \equiv \sqrt{W_0 w_{\max}}$ (cf. equation [24]), so

that in terms of the function $\ln w(\zeta)$, the point $\zeta_{1/2}$ corresponds to the FWHM. The quantity $V_{1/2}$ can thus be obtained from the following equation

$$2\int_0^{V_{1/2}} dV/\sqrt{R(V)} = \int_0^{V_1} dV/\sqrt{R(V)} + \int_{V_0}^{V_1} dV/\sqrt{R(V)} \tag{B2}$$

In the case of a weak CRC, $\Pi \ll 1$, we obviously have $V_{1/2} < V_0 \sim V_1 \ll 1$, so that substituting R from equation (16), we have

$$\mathrm{erfc}\left(\ln\frac{1}{V_{1/2}} - \frac{q}{2}\right) = \frac{1}{2}$$

or

$$V_{1/2} = e^{-\frac{q}{2}-\sigma} = V_0 e^{-\sigma} \approx V_1 e^{-\sigma}/\left(1+\frac{1}{2}e^{-q}\right)$$

where $\mathrm{erfc}(\sigma) = 1/2$, so that $\sigma \approx 0.48$. Substituting then $V_{1/2}$ into $\zeta_{1/2}$ from equation (A4) we obtain the result given by equation (26).

In the case $\Pi \gg 1$, the integrals on the r.h.s. of Equation (B2) are dominated by the upper limit, so the integral on the l.h.s. must also be and we deduce $V_{1/2} \approx V_1$, from which we obtain the nonlinear CR half-life in Equation (28).

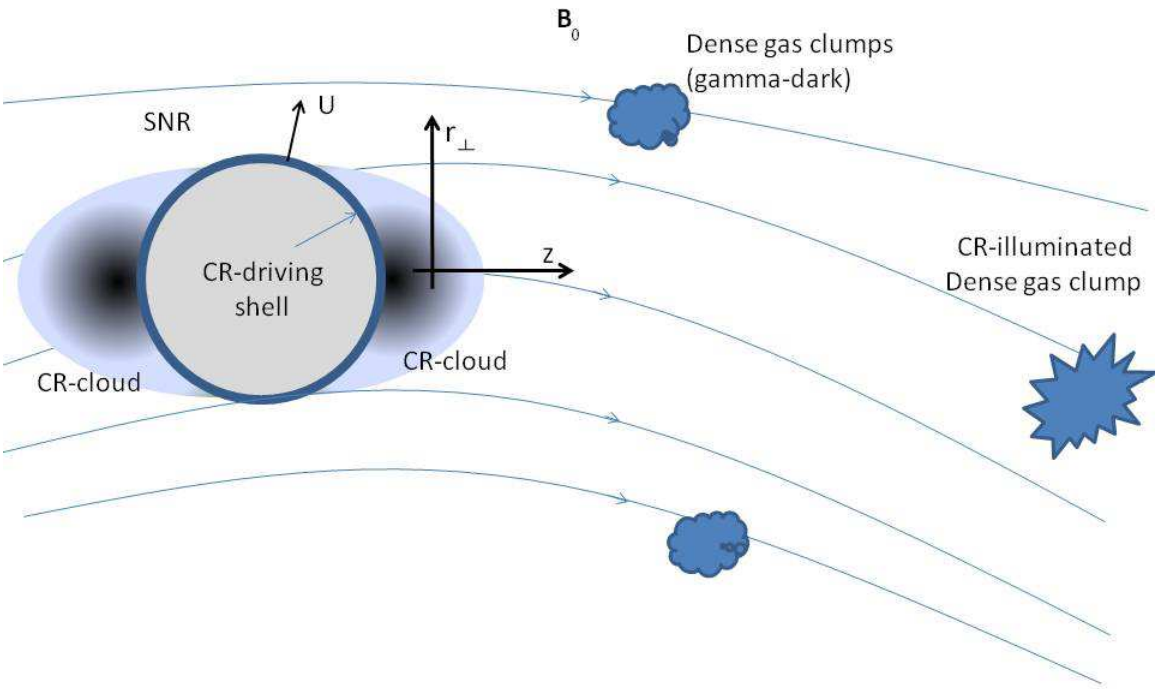


Fig. 1.— CR escape along the magnetic field $\mathbf{B}_0$ from the two polar cusps of SNR with a stalled blast wave.

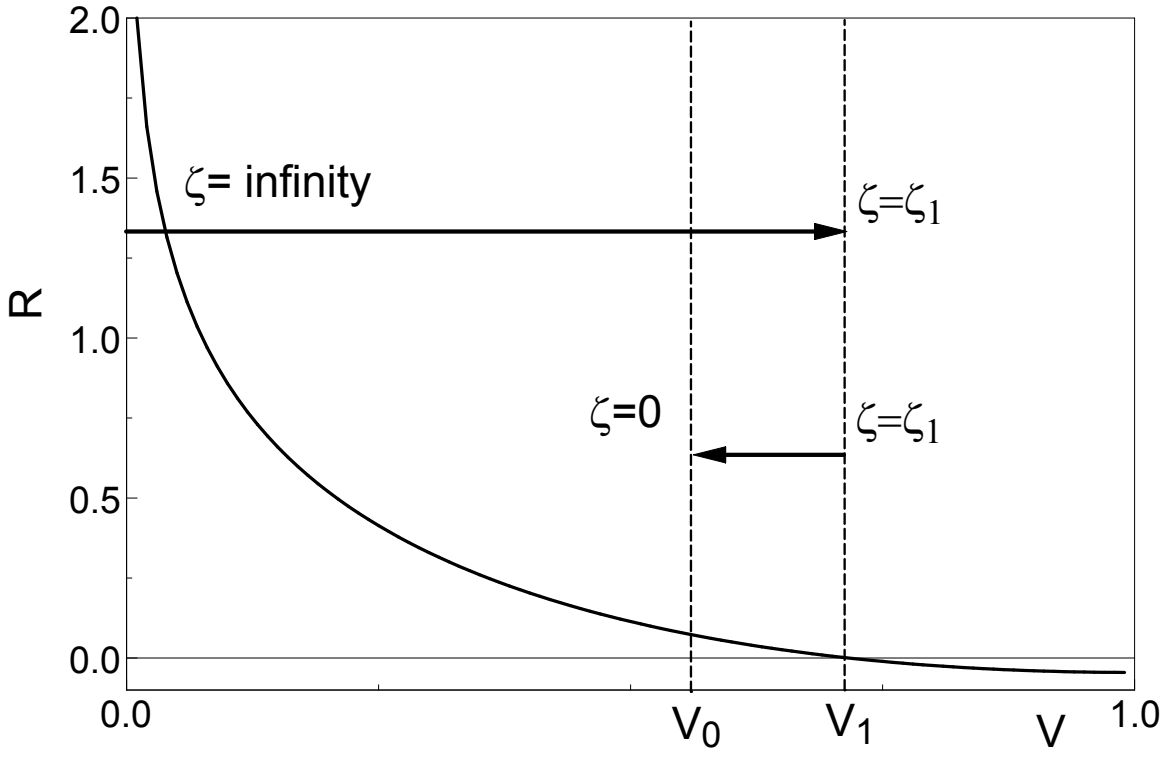


Fig. 2.— Function $R(V)$ and the limits of integration in equations (17) and (A1) depicted for $\varepsilon = 0.3$.

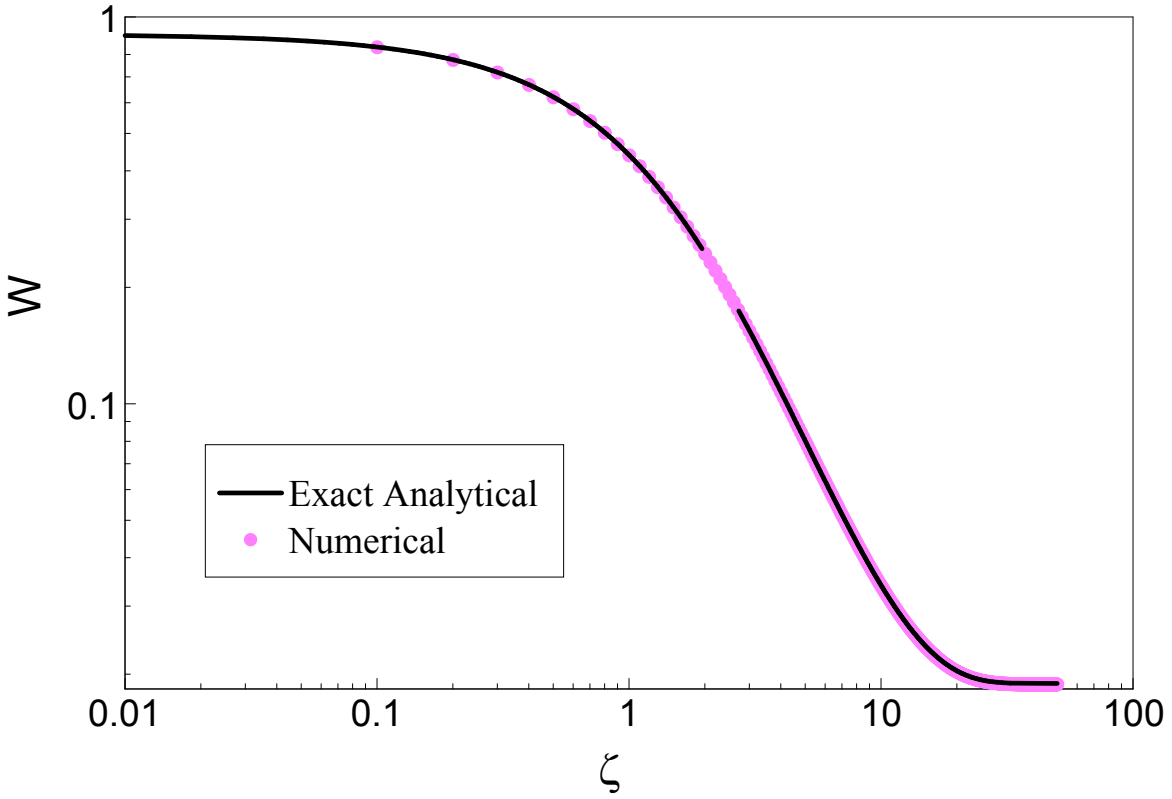


Fig. 3.— Analytic vs numerical solution of eq.(14). The gap in the analytical curve encloses the branching point of the solution at $V = V_1$, eq.(A1). $w_0 = 0.19$, $w_m = 0.9$

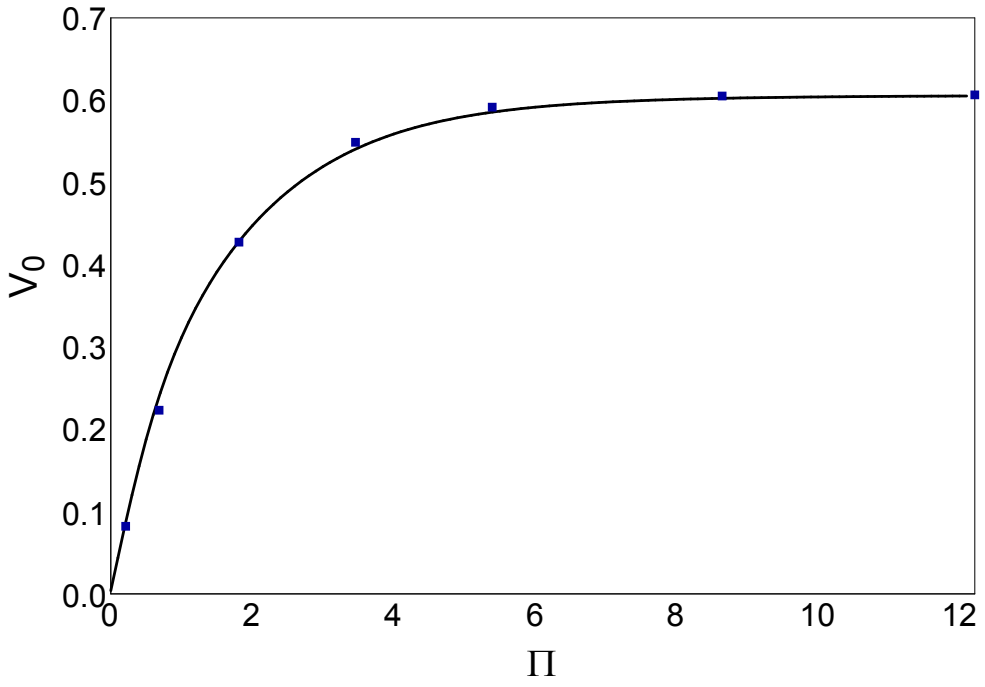


Fig. 4.— Squares: Function $V_0(\Pi)$, obtained from Equation (24). Line: interpolation given by Equation (32).

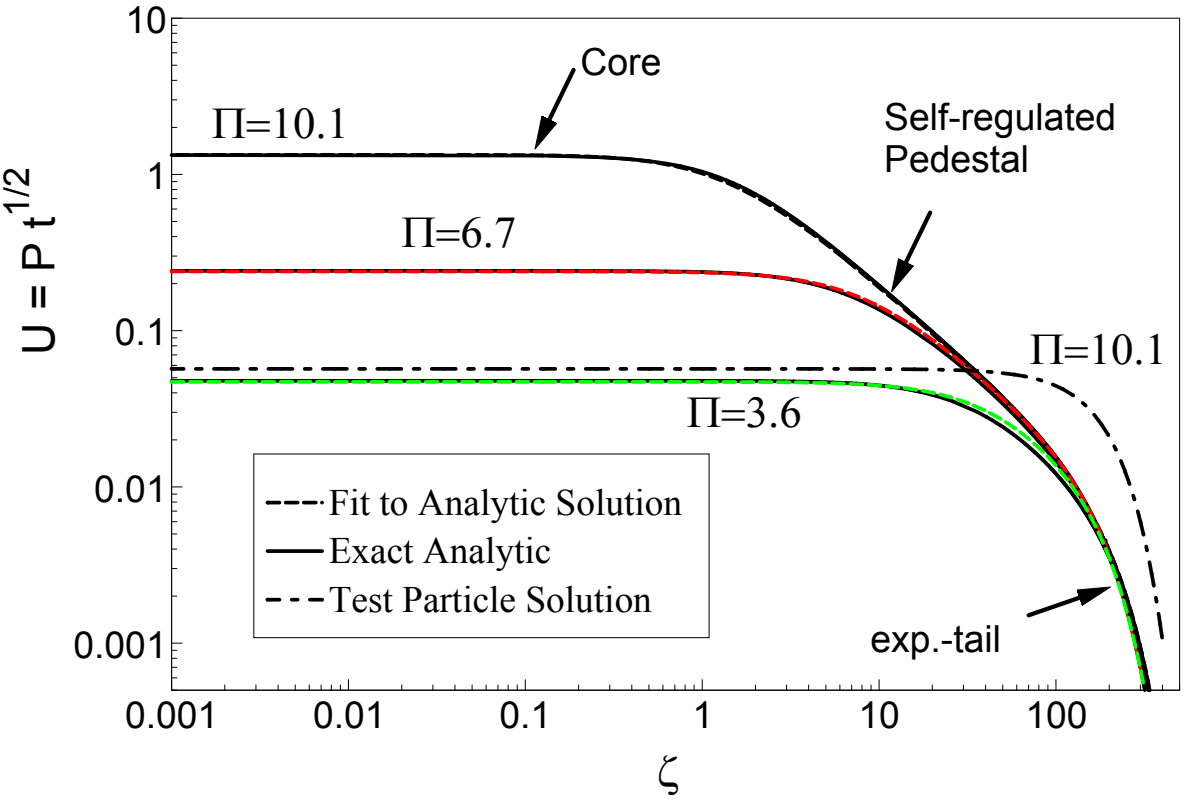


Fig. 5.— Spatial distribution of CR partial pressure (as a function of $\zeta = z/\sqrt{t}$, multiplied by $\sqrt{t}$) shown for integrated values of this quantity $\Pi = 3.6$; 6.7; 10.1 and for for the background wave amplitude $W_0 = 10^{-4}$. Exact analytic solutions are shown with the solid lines while the interpolations given by Equation (38) are shown with the dashed lines. For comparison, a formal linear solution for $\Pi = 10.1$ is also shown with the dot-dashed line. Note the three characteristic zones of the CR confinement: the innermost flat top core, the scale invariant $(1/\zeta)$ pedestal, and the exponential decay zone.

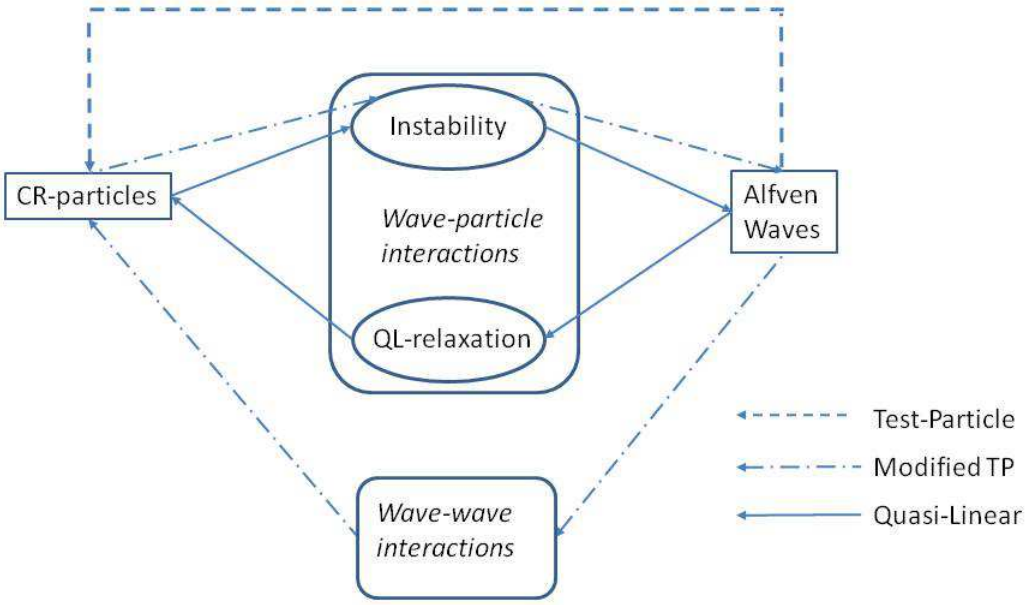


Fig. 6.— Three different approximations for studying injection of accelerated CRs into ISM: Test particle (TP), modified TP (with unstable wave growth and nonlinear wave evolution), and quasi-linear (QL) (with self-consistent time dependent wave-particle interactions).

REFERENCES

Abdo, A. A., M. Ackermann, M. Ajello, A. Allafort, L. Baldini, J. Ballet, G. Barbiellini, D. Bastieri, K. Bechtol, R. Bellazzini, B. Berenji, R. D. Blandford, *et al.*, 2010a, *Astrophys. J.* **718**, 348.

Abdo, A. A., M. Ackermann, M. Ajello, L. Baldini, J. Ballet, G. Barbiellini, M. G. Baring, D. Bastieri, B. M. Baughman, K. Bechtol, R. Bellazzini, B. Berenji, *et al.*, 2010b, Science **327**, 1103.

Abdo, A. A., M. Ackermann, M. Ajello, L. Baldini, J. Ballet, G. Barbiellini, D. Bastieri, B. M. Baughman, K. Bechtol, R. Bellazzini, B. Berenji, R. D. Blandford, *et al.*, 2010c, *Astrophys. J.* **712**, 459.

Achterberg, A., 1981, Astronomy and Astrophys. **98**, 161.

Aharonian, F., A. G. Akhperjanian, A. R. Bazer-Bachi, B. Behera, M. Beilicke, W. Benbow, D. Berge, K. Bernlöhr, C. Boisson, O. Bolz, V. Borrel, I. Braun, *et al.*, 2008, Astronomy and Astrophys. **481**, 401.

Aharonian, F. A., and A. M. Atoyan, 1996, Astronomy and Astrophys. **309**, 917.

Aharonian, F. A., L. O. Drury, and H. J. Voelk, 1994, Astronomy and Astrophys. **285**, 645.

Aleksić, J., E. A. Alvarez, L. A. Antonelli, P. Antoranz, M. Asensio, M. Backes, U. Barres de Almeida, J. A. Barrio, D. Bastieri, J. Becerra González, W. Bednarek, K. Berger, *et al.*, 2012, Astronomy and Astrophys. **541**, A13.

Bell, A. R., 1978, *Mon. Not. R. Astron. Soc.* **182**, 147.

Bell, A. R., 2004, *Mon. Not. R. Astron. Soc.* **353**, 550.

Berezhko, E. G., 1996, Astroparticle Physics **5**, 367.

Bisnovatyi-Kogan, G. S., and S. A. Silich, 1995, Reviews of Modern Physics **67**, 661.

Blasi, P., and E. Amato, 2012, J. Cosmology Astropart. Phys. **1**, 10.

Brunetti, M. T., and A. Codino, 2000, *Astrophys. J.* **528**, 789.

Bykov, A. M., S. M. Osipov, and I. N. Toptygin, 2009, Astronomy Letters **35**, 555.

Diamond, P. H., V. B. Lebedev, D. E. Newman, and B. A. Carreras, 1995, Physics of Plasmas **2**, 3685.

Drury, L. O., 1983, Reports on Progress in Physics **46**, 973.

Drury, L. O., 2011, *Mon. Not. R. Astron. Soc.* **415**, 1807.

Drury, L. O., P. Duffy, D. Eichler, and A. Mastichiadis, 1999, Astronomy and Astrophys. **347**, 370.

Drury, L. O., D. E. Ellison, F. A. Aharonian, E. Berezhko, A. Bykov, A. Decourchelle, R. Diehl, G. Meynet, E. Parizot, J. Raymond, S. Reynolds, and S. Spangler, 2001, Space Science Reviews **99**, 329.

Drury, L. O. C., and S. A. E. G. Falle, 1986, *Mon. Not. R. Astron. Soc.* **223**, 353.

Ellison, D. C., and A. M. Bykov, 2011, *Astrophys. J.* **731**, 87.

Fujita, Y., F. Takahara, Y. Ohira, and K. Iwasaki, 2011, *Mon. Not. R. Astron. Soc.* **415**, 3434.

Funk, S., 2012, ArXiv e-prints 1204.4529.

Gabici, S., 2011, Mem. Soc. Astron. Italiana **82**, 760.

Gabici, S., F. A. Aharonian, and S. Casanova, 2009, *Mon. Not. R. Astron. Soc.* **396**, 1629.

Galinsky, V. L., and V. I. Shevchenko, 2007, *Astrophys. J. Lett.* **669**, L109.

Galinsky, V. L., and V. I. Shevchenko, 2011, *Astrophys. J.* **734**, 106.

Gargaté, L., and A. Spitkovsky, 2012, *Astrophys. J.* **744**, 67.

Giuliani, A., M. Cardillo, M. Tavani, Y. Fukui, S. Yoshiike, K. Torii, G. Dubner, G. Castelletti, G. Barbiellini, A. Bulgarelli, P. Caraveo, E. Costa, *et al.*, 2011, *Astrophys. J. Lett.* **742**, L30.

Gull, S. F., 1973, *Mon. Not. R. Astron. Soc.* **161**, 47.

Hinton, F. L., and G. M. Staebler, 1993, Physics of Fluids B **5**, 1281.

Inoue, T., R. Yamazaki, S.-i. Inutsuka, and Y. Fukui, 2012, *Astrophys. J.* **744**, 71.

Ivanov, A. A., V. D. Rusanov, and R. Z. Sagdeev, 1970, Soviet Journal of Experimental and Theoretical Physics Letters **12**, 20.

Kirk, J. G., and R. O. Dendy, 2001, JOURNAL OF PHYSICS G-NUCLEAR AND PARTICLE **27**, 1589.

Lagage, P. O., and C. J. Cesarsky, 1983, Astronomy and Astrophys. **125**, 249.

Maggi, C. F., 2010, Nuclear Fusion **50**(6), 066001.

Malkov, M. A., and P. H. Diamond, 2006, *Astrophys. J.* **642**, 244.

Malkov, M. A., and P. H. Diamond, 2008, Physics of Plasmas **15**(12), 122301.

Malkov, M. A., P. H. Diamond, and T. W. Jones, 2002, *Astrophys. J.* **571**, 856.

Malkov, M. A., P. H. Diamond, and R. Z. Sagdeev, 2005, *Astrophys. J. Lett.* **624**, L37.

Malkov, M. A., P. H. Diamond, and R. Z. Sagdeev, 2010, Plasma Physics and Controlled Fusion **52**(12), 124006.

Malkov, M. A., P. H. Diamond, and R. Z. Sagdeev, 2011, Nature Communications **2/1195**.

Malkov, M. A., and H. J. Völk, 1995, Astronomy and Astrophys. **300**, 605.

Moskalenko, I. V., T. A. Porter, M. A. Malkov, and P. H. Diamond, 2008, in *International Cosmic Ray Conference*, volume 2 of *International Cosmic Ray Conference*, pp. 763–766.

Ohira, Y., K. Murase, and R. Yamazaki, 2011, *Mon. Not. R. Astron. Soc.* **410**, 1577.

Ptuskin, V. S., and V. N. Zirakashvili, 2005, Astronomy and Astrophys. **429**, 755.

Ptuskin, V. S., V. N. Zirakashvili, and A. A. Plesser, 2008, Advances in Space Research **42**, 486.

Reville, B., J. G. Kirk, and P. Duffy, 2009, *Astrophys. J.* **694**, 951.

Rosner, R., and G. Bodo, 1996, *Astrophys. J. Lett.* **470**, L49.

Ryutov, D. D., and R. Z. Sagdeev, 1970, Soviet Journal of Experimental and Theoretical Physics **31**, 396.

Skilling, J., 1975, *Mon. Not. R. Astron. Soc.* **172**, 557.

Strong, A. W., I. V. Moskalenko, and V. S. Ptuskin, 2007, Annual Review of Nuclear and Particle Science **57**, 285.

Tavani, M., A. Giuliani, A. W. Chen, A. Argan, G. Barbiellini, A. Bulgarelli, P. Caraveo, P. W. Cattaneo, V. Cocco, T. Contessi, F. D'Ammando, E. Costa, *et al.*, 2010, *Astrophys. J. Lett.* **710**, L151.

Torres, D. F., H. Li, Y. Chen, A. Cillis, A. G. Caliandro, and A. Y. Rodríguez-Marrero, 2011, *Mon. Not. R. Astron. Soc.* **417**, 3072.

Truelove, J. K., and C. F. McKee, 1999, *Astrophys. J. Suppl.* **120**, 299.

Uchiyama, Y., S. Funk, H. Katagiri, J. Katsuta, M. Lemoine-Goumard, H. Tajima, T. Tanaka, and D. Torres, 2012, ArXiv e-prints 1203.3234.

Völk, H. J., E. G. Berezhko, and L. T. Ksenofontov, 2003, Astronomy and Astrophys. **409**, 563.

Wagner, F., G. Becker, K. Behringer, D. Campbell, A. Eberhagen, W. Engelhardt, G. Fussmann, O. Gehre, J. Gernhardt, G. V. Gierke, G. Haas, M. Huang, *et al.*, 1982, Physical Review Letters **49**, 1408.

Wentzel, D. G., 1974, ARA&A **12**, 71.

Yan, H., A. Lazarian, and R. Schlickeiser, 2012, *Astrophys. J.* **745**, 140.

Zirakashvili, V. N., and V. S. Ptuskin, 2008, *Astrophys. J.* **678**, 939.

This preprint was prepared with the AAS LaTeX macros v5.2.